HHS Public Access

Author manuscript

Circ Res. Author manuscript; available in PMC 2015 September 12.

Published in final edited form as:

Circ Res. 2014 September 12; 115(7): 650–661. doi:10.1161/CIRCRESAHA.114.304056.

$Ca_V3.2$ Channels and the Induction of Negative Feedback in Cerebral Arteries

Osama F. Harraz[*], **Rasha R. Abd El-Rahman**[*], **Kamran Bigdely-Shamloo**, **Sean M. Wilson**, **Suzanne E. Brett**, **Monica Romero**, **Albert L. Gonzales**, **Scott Earley**, **Edward J. Vigmond**, **Anders Nygren**, **Bijoy K. Menon**, **Rania E. Mufti**, **Tim Watson**, **Yves Starreveld**, **Tobias Furstenhaupt**, **Philip R. Muellerleile**, **David T. Kurjiaka**, **Barry D. Kyle**, **Andrew P. Braun**, and **Donald G. Welsh**

Department of Physiology and Pharmacology, Hotchkiss Brain and Libin Cardiovascular Institutes (O.F.H., R.R.A.E.-R., K.B.-S., S.E.B., R.E.M., B.D.K., A.P.B., D.G.W.), Department of Electrical and Computer Engineering (K.B.-S., E.J.V., A.N.), Department of Clinical Neurosciences (B.K.M., T.W., Y.S.), and Microscopy Imaging Facility (T.F.), University of Calgary, Calgary, Alberta, Canada; Department of Pharmacology and Toxicology, Alexandria University, Alexandria, Egypt (O.F.H.); Division of Pharmacology, Loma Linda University, CA (S.M.W., M.R.); Department of Biomedical Sciences, Colorado State University, Fort Collins (A.L.G.); Department of Pharmacology, University of Nevada, Reno (S.E.); LIRYC Institute and Lab IMB, University of Bordeaux, Bordeaux, France (E.J.V.); and Department of Biomedical Sciences, Grand Valley State University, Allendale, MI (P.R.M., D.T.K.)

Abstract

Rationale—T-type ($Ca_V3.1/Ca_V3.2$) Ca^{2+} channels are expressed in rat cerebral arterial smooth muscle. Although present, their functional significance remains uncertain with findings pointing to a variety of roles.

Objective—This study tested whether $Ca_V3.2$ channels mediate a negative feedback response by triggering Ca^{2+} sparks, discrete events that initiate arterial hyperpolarization by activating large-conductance Ca^{2+}-activated K^+ channels.

Methods and Results—Micromolar Ni^{2+}, an agent that selectively blocks $Ca_V3.2$ but not $Ca_V1.2/Ca_V3.1$, was first shown to depolarize/constrict pressurized rat cerebral arteries; no effect was observed in $Ca_V3.2^{-/-}$ arteries. Structural analysis using 3-dimensional tomography, immunolabeling, and a proximity ligation assay next revealed the existence of microdomains in cerebral arterial smooth muscle which comprised sarcoplasmic reticulum and caveolae. Within these discrete structures, $Ca_V3.2$ and ryanodine receptor resided in close apposition to one another. Computational modeling revealed that Ca^{2+} influx through $Ca_V3.2$ could repetitively activate

Correspondence to: Donald G. Welsh, PhD, Department of Physiology and Pharmacology, GAA-14, Health Research Innovation Center, 3280 Hospital Dr NW Calgary, Alberta T2N-4N1, Canada. dwelsh@ucalgary.

[*]These authors are co-first authors and contributed equally to this article.

The online-only Data Supplement is available with this article at http://circres.ahajournals.org/lookup/suppl/doi:10.1161/CIRCRESAHA.114.304056/-/DC1.

Disclosures

None.

ryanodine receptor, inducing discrete Ca^{2+}-induced Ca^{2+} release events in a voltage-dependent manner. In keeping with theoretical observations, rapid Ca^{2+} imaging and perforated patch clamp electrophysiology demonstrated that Ni^{2+} suppressed Ca^{2+} sparks and consequently spontaneous transient outward K^+ currents, large-conductance Ca^{2+}-activated K^+ channel mediated events. Additional functional work on pressurized arteries noted that paxilline, a large-conductance Ca^{2+}-activated K^+ channel inhibitor, elicited arterial constriction equivalent, and not additive, to Ni^{2+}. Key experiments on human cerebral arteries indicate that $Ca_V3.2$ is present and drives a comparable response to moderate constriction.

Conclusions—These findings indicate for the first time that $Ca_V3.2$ channels localize to discrete microdomains and drive ryanodine receptor–mediated Ca^{2+} sparks, enabling large-conductance Ca^{2+}-activated K^+ channel activation, hyperpolarization, and attenuation of cerebral arterial constriction.

Keywords

calcium channels; calcium channels, T-type; calcium signaling; cerebral arteries; muscle, smooth, vascular; potassium channels, calcium-activated; vasodilation

Cerebral arteries form an integrated network that controls the magnitude and distribution of tissue blood flow. Tone within these structures is regulated by multiple stimuli including blood flow,[1,2] neuronal activity,[3,4] tissue metabolism,[5] and intraluminal pressure.[6] These vasoactive stimuli alter myosin light chain phosphorylation through a dynamic process controlled by myosin light chain kinase and phosphatase.[7–9] Although the precise signaling mechanisms do vary among stimuli, a global rise in cytosolic $[Ca^{2+}]_i$ is generally thought to be a key mediating step.[6] This global rise is in turn intimately tied to changes in the smooth muscle membrane potential (V_M) and the subsequent activation of voltage-gated Ca^{2+} channels.[6,10,11]

Voltage-gated Ca^{2+} channels are heteromultimeric complexes that comprise a pore-forming α_1 subunit and auxiliary subunits that influence gating and protein trafficking to the plasma membrane.[12] In cerebral arterial smooth muscle, the L-type $Ca_V1.2$ channel is the dominant Ca^{2+} entry pathway by which vasoactive stimuli set cytosolic $[Ca^{2+}]_i$ and consequently tone development.[6,13] Recent studies have noted that, in addition to $Ca_V1.2$, T-type channels (ie, $Ca_V3.1$ and $Ca_V3.2$) are also expressed in rat and mouse cerebral arteries.[14–16] It has been argued that the T-type conductance, like that of $Ca_V1.2$, plays a direct role in elevating cytosolic $[Ca^{2+}]_i$, albeit at hyperpolarized potentials attributable to a leftward shift in their voltage dependence.[14,15,17] Earlier reports have, however, suggested that the relationship between T-type channels and arterial tone is more complex with Ca^{2+} influx via $Ca_V3.2$ potentially acting in a discrete fashion to influence a defined target. Speculation of the downstream effector does vary, ranging from nitric oxide synthase in the endothelium to Ca^{2+}-activated channels in the smooth muscle.[18–20]

The large-conductance Ca^{2+}-activated K^+ channel (BK_{Ca}) is expressed in cerebral arterial smooth muscle, and its principal role is to feedback upon and limit excessive constriction. [21,22] Vasoconstrictor stimuli enhance BK_{Ca} activity through arterial depolarization and augmentation of Ca^{2+} spark generation. Ca^{2+} sparks are discrete

sarcoplasmic reticulum (SR)–driven events that arise in response to the transient opening of ryanodine receptors (RyRs).[23] Although the functional significance of Ca^{2+} sparks is recognized,[22–24] the mechanistic events that initiate repetitive SR release remain ambiguous, with current theories suggesting a role for $Ca_V1.2$ or transient receptor potential vanilloid 4 channel in triggering the cytosolic or luminal gate of RyR.[25–27] Decidedly absent from this discussion has been a potential role for a T-type conductance.

The present study tested whether $Ca_V3.2$ channel triggers Ca^{2+} spark generation, BK_{Ca} channel activation, and ultimately negative feedback control of cerebral arterial tone. Our examination progressed from cellular to tissue level and involved the integrative use of pressurized vessel myography, electrophysiology, confocal and electron microscopy, and computational modeling. In rat cerebral arteries, we specifically show that $Ca_V3.2$ and RyR colocalize within a microdomain and that steady-state depolarization activates $Ca_V3.2$ to trigger Ca^{2+} sparks. We subsequently show that $Ca_V3.2$-evoked Ca^{2+} sparks activate BK_{Ca} channels, contributing to hyperpolarization that attenuates myogenic constriction. We further demonstrate that this negative feedback mechanism is not limited to rat arteries but extends to the human cerebral circulation. Overall, this study is the first to illustrate that localized Ca^{2+} influx through T-type Ca^{2+} channels in vascular smooth muscle plays an important but indirect role in setting arterial tone by targeting key conductances involved in V_M regulation.

Materials and Methods

Female Sprague Dawley rats were euthanized by CO_2 asphyxiation as approved by the Animal Care and Use Committee at the University of Calgary. Rat brains were removed, placed in cold PBS, and middle and posterior cerebral arteries were isolated. Human cerebral arteries were extracted from resected brain tissue according to the University of Calgary Institutional Review Board. Structural analysis was performed using confocal, electron, and epifluorescence approaches. Vasomotor/V_M responses were subsequently assessed with the aid of pressure myography. Conventional, perforated, and on-cell patch clamp electrophysiology was used to record whole-cell and single-channel voltage-gated Ca^{2+} and BK_{Ca} currents. Data are presented as means ± SEM; paired or unpaired *t* tests were performed where appropriate, and a $P<0.05$ was considered statistically significant. An expanded version of the Materials and Methods can be found in the Online Data Supplement.

Results

$Ca_V3.2$ Inhibition: Vasomotor and Electric Responses in Rat Cerebral Arteries

Our examination began by confirming the ability of 50 μmol/L Ni^{2+} or 200 nmol/L nifedipine to block $Ca_V3.2$ and $Ca_V1.2$ currents, respectively, in tSA-201 cells. Figure 1A illustrates that Ni^{2+} effectively abolished inward Ba^{2+} current through $Ca_V3.2$ channels without affecting charge movement through $Ca_V1.2$ or $Ca_V3.1$ (Online Figure I). In comparison, nifedipine selectively blocked $Ca_V1.2$ channels (Online Figure I). Moving to rat cerebral arterial smooth muscle cells, we next monitored the nifedipine-insensitive Ba^{2+} current, a conductance that is dominated by T-type channels and is stable over time (Online

Figure IIA and IIB).[28,29] Nickel partially attenuated this native inward current, a finding consistent with $Ca_V3.2$ channel expression (Figure 1B). On-cell recordings further denoted T-type activity in rat cerebral arterial smooth muscle. While $Ca_V1.2$ channels were blocked, single-channel activity was observed at hyperpolarized voltages (−50 to −20 mV), and slope conductance was 8.5 pS. The subsequent application of Ni^{2+} to endothelial-denuded arteries enhanced myogenic tone at 20 to 80 mm Hg (Figure 1C and 1D). Control experiments confirmed that arterial responses to pressure were repeatable over time (Online Figure IIC). Coincident with arterial constriction was an Ni^{2+}-induced depolarization of 5 ± 0.9 mV in pressurized arteries (Figure 1E and 1F). The latter observation inferred that $Ca_V3.2$-mediated Ca^{2+} influx could elicit hyperpolarization and dilation through a smooth muscle signaling mechanism. In theory, this hyperpolarization could be triggered through localized Ca^{2+} entry initiating RyR-mediated Ca^{2+} sparks, SR events that activate BK_{Ca} channels.[18,19,23] Nickel's effects on the nifedipine-insensitive Ba^{2+} current and arterial tone were reversible (not shown).

Microdomains and the Colocalization of $Ca_V3.2$ and RyR

$Ca_V3.2$ and RyR reside in the plasma and SR membranes, respectively. For these proteins to functionally interact, there must be regions where the 2 membranes come into close apposition. With this in mind, 3-dimensional electron tomography assayed for microdomains; image analysis and model reconstruction revealed the presence of microstructures which comprised caveolae and SR (Figure 2A–2C). These discrete regions were ≈500 to 600 nm in length and were circumferentially discontinuous. Immunogold labeling subsequently confirmed that RyR localized to regions underneath caveolae, whereas $Ca_V3.2$ was confined to the plasma membrane in-or-close to caveolae (Figure 2D–2F).

To strengthen the emerging relationship between $Ca_V3.2$ and RyR, the preceding structural work was supplemented with an immunohistochemical analysis of fixed cerebral arteries using antibodies against actin, $Ca_V3.2$, and RyR. Findings in Figure 3A first illustrate that actin labeling runs lengthwise in cerebral arterial smooth muscle cells, fading every 7 to 10 μm as actin leaves the viewing plane. $Ca_V3.2$ staining was circumferential and often observed in regions devoid of smooth muscle actin. A similar circumferential pattern was observed for RyR2, a finding indicative although not definitive for colocalization with $Ca_V3.2$ (Figure 3B). Unlike $Ca_V3.2$ and RyR, $Ca_V1.2$ labeling was ribbon-like and ran lengthwise in smooth muscle (Figure 3C). A proximity ligation assay was subsequently performed, and consistent with $Ca_V3.2$ and RyR2 residing within 40 nm of one another, punctate red fluorescent product was observed in myocytes treated with both primary and secondary antibodies (Figure 4A). Reaction product was absent in control experiments where one or both primary antibodies were removed (Figure 4B–4D).

$Ca_V3.2$, RyR-Mediated Ca^{2+} Release, and the Induction of BK_{Ca} Activity

To ascertain at a conceptual level whether Ca^{2+} flux through $Ca_V3.2$ channels could activate RyR to initiate Ca^{2+} sparks, a computational model was designed. The microdomain model (Figure 5A) was developed based on the preceding structural data, measurements of Ca_V channel activity, and mathematical representations of other Ca^{2+} transporters/binding proteins. Findings illustrate that a depolarizing stimulus (from −60 to −40 mV) elicits Ca^{2+}

spark-like events in the subspace between the plasma membrane and the SR (Figure 5B). These repetitive events fire at a frequency of ≈0.11 Hz and are fully abolished with RyR blockade (Figure 5C). In keeping with a role for $Ca_V3.2$, the elimination of this conductance attenuated these spark-like events (≈59% inhibition, Figure 5D). A broader voltage-dependent analysis also revealed that the frequency of Ca^{2+} spark-like events rose with depolarization (Figure 5E).

Moving forward to experimentally explore the $Ca_V3.2$/RyR relationship, Ca^{2+} imaging and line scan analysis were used to monitor Ca^{2+} sparks in rat cerebral arteries (Figure 6A). In opened tissues, Ca^{2+} sparks were observed in 57% of 291 line scans with a mean frequency of 0.0148 sparks/μm per second. Subsequent application of Ni^{2+} reduced event frequency by 53% (Figure 6A–6C) and had a significant effect on the spatial/temporal characteristics of Ca^{2+} sparks (Online Figure III). Given these positive observations, we next used perforated patch clamp electrophysiology to monitor spontaneous transient outward K^+ currents (STOCs), BK_{Ca}-mediated events in response to Ca^{2+} spark generation.[21–23] Findings in Figure 6D show that STOCs were robustly observed in cerebral arterial myocytes and their frequency increased as the holding V_M was stepped from −40 to −20 mV. The subsequent application of 50 μmol/L Ni^{2+} reduced STOC frequency at −40 but not −20 mV, a finding consistent with the voltage dependence of $Ca_V3.2$ channels. The reduction in STOC frequency occurred without effect on amplitude (Figure 6D). In comparison, STOCs were abolished by 1 μmol/L paxilline, a BK_{Ca} inhibitor (Figure 6E). Control experiments (Online Figure IV) confirmed that peak inward/outward current in myocytes, slowly ramped from −60 to +20 mV, was unaffected by Ni^{2+}. They also confirmed that 200 nmol/L nifedipine does not reduce STOC frequency at −40 mV (n=4: control, 70 ± 15 events/min; nifedipine, 62 ± 12 events/min). Overall, these results support the view Ca^{2+} influx via $Ca_V3.2$ channels drives BK_{Ca} activity via a mechanism involving RyR and the induction of Ca^{2+} sparks.

Further functional experiments were sought to emphasize the relationship between $Ca_V3.2$, BK_{Ca} activity, and the attenuation of arterial constriction. First, Figure 7A and 7B reveals that BK_{Ca} blockade (paxilline, 1 μmol/L) enhanced myogenic tone at intravascular pressures <80 mm Hg, akin to Ni^{2+} (Figure 1C and 1D). Second, when Ni^{2+} and paxilline were sequentially added, the first agent induced constriction, whereas the second had little or no additional effect (Figure 7C–7F). Control experiments confirmed that Ni^{2+}-induced constriction at 60 mm Hg was absent in mesenteric arteries isolated from $Ca_V3.2^{-/-}$ mice (Figure 7G and 7H). Overall, these results are consistent with $Ca_V3.2$ and BK_{Ca} channels working cooperatively within a common signaling pathway.

$Ca_V3.2$ in Human Cerebral Arteries

A final set of experiments was conducted on human cerebral arteries to ascertain the translational impact of the preceding findings. Cerebral arteries were isolated from brain tissues resected from patients undergoing temporal lobectomy (Figure 8A). Polymerase chain reaction analysis on isolated smooth muscle cells, prescreened for endothelial contamination, illustrated that $Ca_V3.2$ mRNA was expressed (Figure 8B). Whole-cell patch clamp electrophysiology subsequently confirmed the presence of a nifedipine-insensitive current that was partially sensitive to 50 μmol/L Ni^{2+} (Figure 8C). Analogous to rat, Ni^{2+}

application to human cerebral arteries elicited constriction and enhanced myogenic tone at pressure values ≤60 mm Hg (Figure 8D and 8E). These findings confirm that $Ca_V3.2$ is not only expressed in human myocytes, but its paradoxical role in tone development is likely akin to the rat.

Discussion

This study delineated $Ca_V3.2$ channels in cerebral arterial smooth muscle and determined whether this T-type conductance triggers Ca^{2+} sparks and consequently BK_{Ca} channels to elicit feedback control of arterial tone. Experiments progressed from cells to tissues and incorporated electrophysiology, cellular imaging, and computational modeling. Patch clamp electrophysiology confirmed the presence of a $Ca_V3.2$ current in cerebral arterial smooth muscle cells, a conductance selectivity blocked by micromolar Ni^{2+}. In pressurized arteries, $Ca_V3.2$ blockade induced unexpected depolarization and constriction, a result indicative of $Ca_V3.2$ involvement in a dilatory process. A combination of structural and protein localization techniques revealed that $Ca_V3.2$ channels localize to microdomains in close apposition to RyR. Computational modeling then conceptually revealed that $Ca_V3.2$ could gate RyR, elicit Ca^{2+} sparks, and activate BK_{Ca} channels. Consistent with these predictions, Ni^{2+} inhibited Ca^{2+} spark production and STOC generation at physiological voltages. Further functional analysis reinforced this linkage by extending experiments to humans. In summary, this study is the first to demonstrate that $Ca_V3.2$ drives a local Ca^{2+}-induced Ca^{2+} release event that restrains cerebral arterial constriction by triggering Ca^{2+} sparks and BK_{Ca} channel activation.

Background

The depolarization of cerebral arterial smooth muscle augments extracellular Ca^{2+} influx through the activation of voltage-gated Ca^{2+} channels. This response elevates global $[Ca^{2+}]_i$, enhances myosin light chain phosphorylation, and augments arterial tone development.[6,9] Ca^{2+} channels are categorized according to the pore-forming α_1–subunit,[12] and in cerebral arterial smooth muscle, the L-type $Ca_v1.2$ is considered the primary conductance governing Ca^{2+} entry.[6] Although $Ca_V1.2$ is a dominant conductance, recent studies have begun to acknowledge the expression of low-voltage activated Ca^{2+} channels in cerebral arteries.[14,15,28] T-type channels are the sole members of this subfamily, and as their name suggests, their activation/inactivation profiles are leftward shifted compared with the high-voltage activated L-type Ca^{2+} channels.[12,28] $Ca_V3.1$ and $Ca_V3.2$ are expressed in arterial smooth muscle, and recent work suggests that Ca^{2+} entry through one or both T-type channels could elevate global $[Ca^{2+}]_i$, albeit at more hyperpolarized potentials, to modestly facilitate myogenic tone.[14–17,29] Although Ca^{2+} entry through T-type channels could drive bulk $[Ca^{2+}]_i$ changes, it could also elicit localized increases to gate conductances tied to V_M regulation.[18,19] To date, evidence of discrete Ca^{2+} signaling is limited in vascular tissue although studies have alluded to this possibility given the unexpected impairment of arterial dilation after $Ca_V3.2$ blockade.[19,30]

$Ca_V3.2$ Channels in Cerebral Arteries

Studying vascular T-type channels is challenging because pharmacological tools display minimal subtype selectivity. The one exception is Ni^{2+} which, at low micromolar concentrations, selectively blocks $Ca_V3.2$ over $Ca_V3.1$ or $Ca_V1.2$, the primary Ca^{2+} channels in vascular smooth muscle.[28,31] We confirmed Ni^{2+} selectivity by transfecting the preceding $Ca_Vx.x$ subunits into tSA-201 cells and monitoring the inward Ba^{2+} current (Figure 1; Online Figure I). Moving into cerebral arterial myocytes and focusing on the nifedipine-insensitive current dominated by T-type activity, [28,29] Ni^{2+} attenuated but did not abolish this conductance, consistent with expression of both $Ca_V3.2$ and $Ca_V3.1$. On-cell electrophysiology further confirmed successful single-channel recordings with a slope conductance consistent with T-type channels.[32] Although only a handful of vascular studies have exploited differential Ni^{2+} sensitivity to isolate $Ca_V3.2$ currents,[19,28,33] this approach is commonly used in cardiac/neuronal tissues to isolate this conductance and to ascertain its cellular function.[34,35] In this context, we show for the first time that selective $Ca_V3.2$ blockade augmented myogenic tone, findings paradoxical to typical vasodilatory effects of Ca^{2+} channel blockers.[6,14,15] The enhancement of tone resulted from the ability of Ni^{2+} to depolarize arterial V_M. These observations along with earlier reports[19] indicate that $Ca_v3.2$ might elicit localized rise in cytosolic $[Ca^{2+}]_i$ that gates a K^+ conductance that limits arterial constriction.

In the cerebral circulation, BK_{Ca} channels moderate vasoconstriction to agonists and elevated intravascular pressure. The channel comprises 4 pore-forming α_1-subunits and 4 β_1-subunits to confer Ca^{2+} sensitivity.[24,36] To activate BK_{Ca}, $[Ca^{2+}]_i$ must discretely rise to micromolar levels and this is achieved through Ca^{2+} spark generation, SR events dependent on RyR gating.[21,22,24] The opening of RyR is an integrated process, partially reliant on extracellular Ca^{2+} entry triggering the RyR cytosolic Ca^{2+} sensor. The identity of this entry channel is uncertain although past studies have alluded to candidates including transient receptor potential vanilloid 4 channel[25] and L-type channels.[26,27,37] Although both are plausible candidates, their intrinsic properties are somewhat inconsistent with a triggering role. Transient receptor potential vanilloid 4 channel displays voltage-independent properties, yet Ca^{2+} spark generation is graded in a voltage-dependent manner. L-type channels exhibit Ca^{2+}-dependent inactivation and if positioned in a diffusion-restriction microdomain, high $[Ca^{2+}]_i$ would elicit strong inactivation, impinging on its ability to activate the RyR cytosolic gate. Because $Ca_V3.2$ channels are voltage gated, free of Ca^{2+}-dependent inactivation, and display a voltage window that overlaps with physiological V_M,[12,28] this conductance seems best suited for microdomain localization and functioning as a trigger of Ca^{2+}-induced Ca^{2+} release.

Microdomains and Ca^{2+} Channel Localization

For Ca^{2+} influx via $Ca_V3.2$ to trigger RyR and initiate Ca^{2+} sparks, the SR and plasma membranes must form a discrete signaling domain and then the proteins of interest must localize in close apposition to one another. In this context, we began our examination of a potential $Ca_V3.2$– RyR relationship using electron tomography, a structural technique that permits intercellular structures to be viewed in high 3-dimensional resolution. With this approach, microdomains that comprised caveolae and SR were readily identified (Figure 2).

These discrete signaling regions were observed periodically along smooth muscle cells and were discontinuous longitudinally and circumferentially. Immunogold labeling subsequently placed $Ca_V3.2$ in-or-near caveolae and RyR in regions beneath these invaginated structures. In light of these findings, a broader immunohistochemical analysis was performed in which further evidence of $Ca_V3.2$–RyR colocalization was observed. First, using whole-mounted cerebral arteries, this study found that both Ca^{2+} pores were expressed in regions devoid of smooth muscle actin (Figure 3). Their circumferential labeling pattern was intriguing and strikingly distinct from $Ca_V1.2$. Second, a proximity ligation assay yielded a fluorescent product in isolated cells, consistent with $Ca_V3.2$ and RyR2 colocalizing within 40 nm of one another (Figure 4). Immunolabeling controls were negative, and antibody specificity was characterized, a priori, by Western blot analysis.[14]

$Ca_V3.2$ Channels, Ca^{2+} Sparks, STOCs, and Arterial Tone Development

To forward the stated hypothesis, it is important to consider Ca^{2+} flux in context with channel localization and the spatial compartments. Accordingly, our next step was to build a computational model to ascertain whether Ca^{2+} flux through $Ca_V3.2$ could, on a theoretical level, trigger the opening of RyR (Figure 5). Simulations revealed that at physiological V_M, Ca^{2+} spark-like events could be repetitively generated. Event frequency was coupled to voltage, an observation that aligns with experimental literature.[23,38,39] RyR blockade abolished these events, whereas $Ca_v3.2$ inhibition reduced frequency by 59%. In keeping with theory, analysis of opened arteries confirmed that $Ca_V3.2$ blockade decreased the frequency of Ca^{2+} spark (Figure 6); it also had a significant effect on their spatial/temporal characteristics (Online Figure III). The inability of Ni^{2+} to completely block discrete events indicates a complexity to RyR gating that extends beyond our focused analysis of $Ca_v3.2$. Future studies will need to consider whether other Ca^{2+} transporters are present in microdomains and able to trigger the cytosolic Ca^{2+} gate of RyR. Ca^{2+} transport proteins external to the microdomain could also foster Ca^{2+} sparks generation by altering SR refilling or the rate of Ca^{2+} diffusion from the subspace.[26,27]

The predicted consequence of Ni^{2+} blockade and reduced Ca^{2+} spark generation should be decreased BK_{Ca} activity. We assessed the latter using perforated patch clamp electrophysiology to monitor STOCs in arterial myocytes. As denoted in Figure 6D and 6E, Ni^{2+} application reduced STOC frequency at physiological voltages (−40 mV) and had an insignificant effect at depolarized potentials where $Ca_v3.2$ channels reside in the inactive state. In comparison, paxilline abolished all STOC activity at both voltages. The voltage-dependent effect of Ni^{2+} is intriguing, and one that suggests that the ability of $Ca_V3.2$ to drive a feedback response might be confined to a specific V_M range. Functional observations in Figure 1 align with this perspective in that the Ni^{2+} effect on myogenic was greatest at intravascular pressures (40–60 mm Hg) where arterial V_M will overlap with the peak window current of $Ca_V3.2$. Given that paxilline augmented myogenic tone in an analogous manner to Ni^{2+}, we can further suggest that $Ca_V3.2$ channels are likely a dominant trigger of BK_{Ca} in intact cerebral arteries (Figure 7). This view is further supported by our observations that placing one blocker on another had no additive effect on arterial tone.

In interpreting the preceding findings, it is important to consider the possible off-target effects of Ni^{2+}. Past studies have noted that under certain conditions this divalent can affect voltage-gated K^+ and depolarizing transient receptor potential currents.[40–43] Two lines of evidence indicate that such off-target effects are minimal in this study. First, electrophysiology revealed that Ni^{2+} had no effect on peak inward/outward current in smooth muscle cells ramped from −60 to 20 mV (Online Figure IV). Second, Ni^{2+} failed to alter tone in paxilline- pretreated cerebral arteries or in vessels isolated from $Ca_V3.2$ knockout mice (Figure 7).

Translation to Humans

Our work in rat cerebral arteries highlights a structural and functional association among $Ca_V3.2$, RyR, and BK_{Ca}, whereby voltage-dependent Ca^{2+} influx drives Ca^{2+} sparks generation and consequently arterial hyperpolarization. Although these foundational observations are unique and provocative, questions remained as to whether they translate to human tissue. In this context, we harvested human cerebral arteries from resection surgeries and repeated key experiments. We show that $Ca_V3.2$ mRNA is indeed present in human cerebral arterial myocytes. Further, $Ca_V3.2$ is functionally expressed because patch clamp electrophysiology delineated a Ni^{2+}-sensitive T-type current. Finally, consistent with $Ca_V3.2$ driving arterial hyperpolarization, we found that Ni^{2+} constricted pressurized human cerebral arteries with an effect peaking at 60 mm Hg, where arterial V_M likely resides at −45 mV. These findings are the first to note T-type Ca^{2+} channel expression in human cerebral circulation and that it has a unique physiological role.

Summary

Vascular Ca^{2+} channels have been targets of investigative interest with $Ca_v1.2$ receiving particular attention given that dihydropyridines induce profound arterial dilation. With the recent isolation of T-type Ca^{2+} channels,[14,28,33] interest has begun to shift toward defining their physiological function. [17,18,33] Vascular studies using blockers that do not discriminate among the T-type subunits have argued that they contribute modestly to global $[Ca^{2+}]_i$ albeit at hyperpolarized potentials.[14,17] The present study challenges this stereotypic view by arguing that Ca^{2+} influx through $Ca_V3.2$ acts in a localized manner to alter Ca^{2+}-sensitive conductances involved in V_M regulation. Although this study focused specifically on $Ca_V3.2$, RyR, and BK_{Ca}, it is intriguing to speculate that $Ca_V3.1$ might also regulate a Ca^{2+}-activated target such as transient receptor potential melastatin 4 channel or transmembrane member 16A channel, a Ca^{2+}-activated Cl^- conductance.[44,45] Both conductances have been identified in arterial smooth muscle and linked to pressure-induced depolarization.[44–46]

In summary, this study delineated $Ca_V3.2$ channels, explored their cellular expression, and examined their relationship to tone development in the cerebral circulation. Our examination used theoretical and experimental approaches from computational modeling to structural analysis, electrophysiology, and pressure myography. $Ca_V3.2$ channels were readily identified, shown to colocalize in microdomains with RyR to initiate Ca^{2+} sparks. These discrete events activate BK_{Ca} channels to facilitate arterial hyperpolarization and drive a feedback response that moderates constrictor events including those initiated by intravascular pressure. Because $Ca_V3.2$ channels are present in other vascular beds,[17,19,20,30]

their feedback mechanism likely extends beyond the cerebral circulation. These findings also provide a straightforward explanation how $Ca_V3.2$ deletion paradoxically affects arterial relaxation.[19,30] This atypical $Ca_V3.2$ vasomotor response entails further attention given the emerging potential use of therapeutic T-type blockers for hypertension, cerebral vasospasm, or pain.[47–49]

Supplementary Material

Refer to Web version on PubMed Central for supplementary material.

Acknowledgments

We thank Dr Gerald Zamponi and Lina Chen for providing $rCa_Vx.x$-transfected cells. We thank Dr Frank Visser for polymerase chain reaction analysis and Dr Ray Turner and Mirna Kruskic for their help in the immunohistochemical analysis.

Sources of Funding

This work was supported by an operating grant from the Canadian Institutes of Health Research (MOP-69088 to D.G. Welsh). D.G. Welsh is an Alberta Innovates-Health Sciences (AIHS) senior scholar and holds a Canada Research Chair. O.F. Harraz is a Vanier Scholar (Canadian Institutes of Health Research) and is supported by salary studentships from Alberta Innovates (AIHS award) and Achievers in Medical Sciences. R.R. Abd El-Rahman was supported by Queen Elizabeth II Scholarship. Imaging was performed in the LLUSM Advanced Imaging and Microscopy Core with support of NSF grant No. MRI-DBI 0923559 to S.M. Wilson and the Loma Linda University School of Medicine. Calcium imaging was also supported in part by USPHS grant HD069746 to S.M. Wilson.

Nonstandard Abbreviations and Acronyms

BK_{Ca}	large-conductance $Ca2^+$-activated K^+ channel
RyR	ryanodine receptor
SR	sarcoplasmic reticulum
STOC	spontaneous transient outward K^+ current
V_M	membrane potential

References

1. Garcia-Roldan JL, Bevan JA. Flow-induced constriction and dilation of cerebral resistance arteries. Circ Res. 1990; 66:1445–1448. [PubMed: 2335036]
2. Bevan JA, Garcia-Roldan JL, Joyce EH. Resistance artery tone is influenced independently by pressure and by flow. Blood Vessels. 1990; 27:202–207. [PubMed: 2242442]
3. Si ML, Lee TJ. Alpha7-nicotinic acetylcholine receptors on cerebral peri-vascular sympathetic nerves mediate choline-induced nitrergic neurogenic vasodilation. Circ Res. 2002; 91:62–69. [PubMed: 12114323]
4. Brayden JE, Bevan JA. Neurogenic muscarinic vasodilation in the cat. An example of endothelial cell-independent cholinergic relaxation. Circ Res. 1985; 56:205–211. [PubMed: 3918803]
5. Filosa JA, Bonev AD, Straub SV, Meredith AL, Wilkerson MK, Aldrich RW, Nelson MT. Local potassium signaling couples neuronal activity to vasodilation in the brain. Nat Neurosci. 2006; 9:1397–1403. [PubMed: 17013381]
6. Knot HJ, Nelson MT. Regulation of arterial diameter and wall [Ca2+] in cerebral arteries of rat by membrane potential and intravascular pressure. J Physiol. 1998; 508(pt 1):199–209. [PubMed: 9490839]

7. Gallagher PJ, Herring BP, Stull JT. Myosin light chain kinases. J Muscle Res Cell Motil. 1997; 18:1–16. [PubMed: 9147985]
8. Johnson RP, El-Yazbi AF, Takeya K, Walsh EJ, Walsh MP, Cole WC. Ca2+ sensitization via phosphorylation of myosin phosphatase targeting subunit at threonine-855 by Rho kinase contributes to the arterial myogenic response. J Physiol. 2009; 587:2537–2553. [PubMed: 19359365]
9. Cole WC, Welsh DG. Role of myosin light chain kinase and myosin light chain phosphatase in the resistance arterial myogenic response to intravascular pressure. Arch Biochem Biophys. 2011; 510:160–173. [PubMed: 21392499]
10. Welsh DG, Nelson MT, Eckman DM, Brayden JE. Swelling-activated cation channels mediate depolarization of rat cerebrovascular smooth muscle by hyposmolarity and intravascular pressure. J Physiol. 2000; 527(pt 1):139–148. [PubMed: 10944177]
11. Welsh DG, Morielli AD, Nelson MT, Brayden JE. Transient receptor potential channels regulate myogenic tone of resistance arteries. Circ Res. 2002; 90:248–250. [PubMed: 11861411]
12. Catterall WA. Voltage-gated calcium channels. Cold Spring Harb Perspect Biol. 2011; 3:a003947. [PubMed: 21746798]
13. Cheng X, Pachuau J, Blaskova E, Asuncion-Chin M, Liu J, Dopico AM, Jaggar JH. Alternative splicing of Cav1.2 channel exons in smooth muscle cells of resistance-size arteries generates currents with unique electrophysiological properties. Am J Physiol Heart Circ Physiol. 2009; 297:H680–H688. [PubMed: 19502562]
14. Abd El-Rahman RR, Harraz OF, Brett SE, Anfinogenova Y, Mufti RE, Goldman D, Welsh DG. Identification of L- and T-type Ca2+ channels in rat cerebral arteries: role in myogenic tone development. Am J Physiol Heart Circ Physiol. 2013; 304:H58–H71. [PubMed: 23103495]
15. Kuo IY, Ellis A, Seymour VA, Sandow SL, Hill CE. Dihydropyridine-insensitive calcium currents contribute to function of small cerebral arteries. J Cereb Blood Flow Metab. 2010; 30:1226–1239. [PubMed: 20125181]
16. Howitt L, Kuo IY, Ellis A, Chaston DJ, Shin HS, Hansen PB, Hill CE. Chronic deficit in nitric oxide elicits oxidative stress and augments T-type calcium-channel contribution to vascular tone of rodent arteries and arterioles. Cardiovasc Res. 2013; 98:449–457. [PubMed: 23436820]
17. Björling K, Morita H, Olsen MF, Prodan A, Hansen PB, Lory P, Holstein-Rathlou NH, Jensen LJ. Myogenic tone is impaired at low arterial pressure in mice deficient in the low-voltage-activated CaV 3.1 T-type Ca(2+) channel. Acta Physiol (Oxf). 2013; 207:709–720. [PubMed: 23356724]
18. Harraz OF, Welsh DG. T-type Ca^{2+} channels in cerebral arteries: approaches, hypotheses, and speculation. Microcirculation. 2013; 20:299–306. [PubMed: 23331671]
19. Chen CC, Lamping KG, Nuno DW, Barresi R, Prouty SJ, Lavoie JL, Cribbs LL, England SK, Sigmund CD, Weiss RM, Williamson RA, Hill JA, Campbell KP. Abnormal coronary function in mice deficient in alpha1H T-type Ca2+ channels. Science. 2003; 302:1416–1418. [PubMed: 14631046]
20. Svenningsen P, Andersen K, Thuesen AD, Shin HS, Vanhoutte PM, Skott O, Jensen BL, Hill C, Hansen PB. T-type Ca channels facilitate NO-formation, vasodilatation and NO-mediated modulation of blood pressure. Pflugers Arch. In press.
21. Pérez GJ, Bonev AD, Patlak JB, Nelson MT. Functional coupling of ryanodine receptors to KCa channels in smooth muscle cells from rat cerebral arteries. J Gen Physiol. 1999; 113:229–238. [PubMed: 9925821]
22. Pérez GJ, Bonev AD, Nelson MT. Micromolar Ca(2+) from sparks activates Ca(2+)-sensitive K(+) channels in rat cerebral artery smooth muscle. Am J Physiol Cell Physiol. 2001; 281:C1769–C1775. [PubMed: 11698234]
23. Jaggar JH, Wellman GC, Heppner TJ, Porter VA, Perez GJ, Gollasch M, Kleppisch T, Rubart M, Stevenson AS, Lederer WJ, Knot HJ, Bonev AD, Nelson MT. Ca2+ channels, ryanodine receptors and Ca(2+)-activated K+ channels: a functional unit for regulating arterial tone. Acta Physiol Scand. 1998; 164:577–587. [PubMed: 9887980]
24. Brenner R, Peréz GJ, Bonev AD, Eckman DM, Kosek JC, Wiler SW, Patterson AJ, Nelson MT, Aldrich RW. Vasoregulation by the beta1 subunit of the calcium-activated potassium channel. Nature. 2000; 407:870–876. [PubMed: 11057658]

25. Earley S, Heppner TJ, Nelson MT, Brayden JE. TRPV4 forms a novel Ca2+ signaling complex with ryanodine receptors and BKCa channels. Circ Res. 2005; 97:1270–1279. [PubMed: 16269659]
26. Essin K, Welling A, Hofmann F, Luft FC, Gollasch M, Moosmang S. Indirect coupling between Cav1.2 channels and ryanodine receptors to generate Ca2+ sparks in murine arterial smooth muscle cells. J Physiol. 2007; 584:205–219. [PubMed: 17673505]
27. Takeda Y, Nystoriak MA, Nieves-Cintrón M, Santana LF, Navedo MF. Relationship between Ca2+ sparklets and sarcoplasmic reticulum Ca2+ load and release in rat cerebral arterial smooth muscle. Am J Physiol Heart Circ Physiol. 2011; 301:H2285–H2294. [PubMed: 21984539]
28. Harraz OF, Welsh DG. Protein kinase A regulation of T-type Ca2+ channels in rat cerebral arterial smooth muscle. J Cell Sci. 2013; 126:2944–2954. [PubMed: 23613468]
29. Harraz OF, Brett SE, Welsh DG. Nitric oxide suppresses vascular voltage-gated T-type Ca2+ channels through cGMP/PKG signaling. Am J Physiol Heart Circ Physiol. 2014; 306:H279–H285. [PubMed: 24240871]
30. Poulsen CB, Al-Mashhadi RH, Cribbs LL, Skøtt O, Hansen PB. T-type voltage-gated calcium channels regulate the tone of mouse efferent arterioles. Kidney Int. 2011; 79:443–451. [PubMed: 21068717]
31. Lee JH, Gomora JC, Cribbs LL, Perez-Reyes E. Nickel block of three cloned T-type calcium channels: low concentrations selectively block alpha1H. Biophys J. 1999; 77:3034–3042. [PubMed: 10585925]
32. Fox AP, Nowycky MC, Tsien RW. Single-channel recordings of three types of calcium channels in chick sensory neurones. J Physiol. 1987; 394:173–200. [PubMed: 2451017]
33. Kuo IY, Howitt L, Sandow SL, McFarlane A, Hansen PB, Hill CE. Role of T-type channels in vasomotor function: team player or chameleon? Pflugers Arch. 2014; 466:767–779. [PubMed: 24482062]
34. Niwa N, Yasui K, Opthof T, Takemura H, Shimizu A, Horiba M, Lee JK, Honjo H, Kamiya K, Kodama I. Cav3.2 subunit underlies the functional T-type Ca2+ channel in murine hearts during the embryonic period. Am J Physiol Heart Circ Physiol. 2004; 286:H2257–H2263. [PubMed: 14988077]
35. Autret L, Mechaly I, Scamps F, Valmier J, Lory P, Desmadryl G. The involvement of Cav3.2/alpha1H T-type calcium channels in excitability of mouse embryonic primary vestibular neurones. J Physiol. 2005; 567:67–78. [PubMed: 15961427]
36. Plüger S, Faulhaber J, Fürstenau M, Löhn M, Waldschütz R, Gollasch M, Haller H, Luft FC, Ehmke H, Pongs O. Mice with disrupted BK channel beta1 subunit gene feature abnormal Ca(2+) spark/STOC coupling and elevated blood pressure. Circ Res. 2000; 87:E53–E60. [PubMed: 11090555]
37. Cheng X, Jaggar JH. Genetic ablation of caveolin-1 modifies Ca2+ spark coupling in murine arterial smooth muscle cells. Am J Physiol Heart Circ Physiol. 2006; 290:H2309–H2319. [PubMed: 16428350]
38. Nelson MT, Cheng H, Rubart M, Santana LF, Bonev AD, Knot HJ, Lederer WJ. Relaxation of arterial smooth muscle by calcium sparks. Science. 1995; 270:633–637. [PubMed: 7570021]
39. Jaggar JH, Stevenson AS, Nelson MT. Voltage dependence of Ca2+ sparks in intact cerebral arteries. Am J Physiol. 1998; 274:C1755–C1761. [PubMed: 9611142]
40. Cheng YM, Fedida D, Kehl SJ. Kinetic analysis of the effects of H+ or Ni2+ on Kv1.5 current shows that both ions enhance slow inactivation and induce resting inactivation. J Physiol. 2010; 588:3011–3030. [PubMed: 20581043]
41. Wang J, Shimoda LA, Sylvester JT. Capacitative calcium entry and TRPC channel proteins are expressed in rat distal pulmonary arterial smooth muscle. Am J Physiol Lung Cell Mol Physiol. 2004; 286:L848–L858. [PubMed: 14672922]
42. Ene FA, Kalmbach A, Kandler K. Metabotropic glutamate receptors in the lateral superior olive activate TRP-like channels: age- and experience-dependent regulation. J Neurophysiol. 2007; 97:3365–3375. [PubMed: 17376850]
43. Luebbert M, Radtke D, Wodarski R, Damann N, Hatt H, Wetzel CH. Direct activation of transient receptor potential V1 by nickel ions. Pflugers Arch. 2010; 459:737–750. [PubMed: 20101408]

44. Bulley S, Neeb ZP, Burris SK, Bannister JP, Thomas-Gatewood CM, Jangsangthong W, Jaggar JH. TMEM16A/ANO1 channels contribute to the myogenic response in cerebral arteries. Circ Res. 2012; 111:1027–1036. [PubMed: 22872152]

45. Earley S, Waldron BJ, Brayden JE. Critical role for transient receptor potential channel TRPM4 in myogenic constriction of cerebral arteries. Circ Res. 2004; 95:922–929. [PubMed: 15472118]

46. Gonzales AL, Garcia ZI, Amberg GC, Earley S. Pharmacological inhibition of TRPM4 hyperpolarizes vascular smooth muscle. Am J Physiol Cell Physiol. 2010; 299:C1195–C1202. [PubMed: 20826763]

47. Abe M, Okada K, Soma M. T-type Ca channel blockers in patients with chronic kidney disease in clinical practice. Curr Hypertens Rev. 2013; 9:202–209. [PubMed: 24479749]

48. Ball CJ, Wilson DP, Turner SP, Saint DA, Beltrame JF. Heterogeneity of L- and T-channels in the vasculature: rationale for the efficacy of combined L- and T-blockade. Hypertension. 2009; 53:654–660. [PubMed: 19237682]

49. François A, Laffray S, Pizzoccaro A, Eschalier A, Bourinet E. T-type calcium channels in chronic pain: mouse models and specific blockers. Pflugers Arch. 2014; 466:707–717. [PubMed: 24590509]

Novelty and Significance

What Is Known?

- T-type ($Ca_V3.1/Ca_V3.2$) Ca^{2+} channels are expressed in cerebral arterial smooth muscle.
- T-type Ca^{2+} channels are thought to mediate arterial tone development although the mechanisms remain uncertain.

What New Information Does This Article Contribute?

- $Ca_V3.2$ channels mediate a paradoxical dilation in pressurized cerebral arteries.
- $Ca_V3.2$ channels are located in microdomains in association with the sarcoplasmic reticulum and ryanodine receptors.
- Ca^{2+} influx through $Ca_V3.2$ channels triggers ryanodine receptors, generates transient Ca^{2+} sparks, and activates large-conductance Ca^{2+}-activated K^+ channels to elicit hyperpolarization.

T-type ($Ca_V3.1/Ca_V3.2$) Ca^{2+} channels are present in rat cerebral arterial smooth muscle, but their functional significance is uncertain. We tested whether $Ca_V3.2$ channels might mediate dilation rather than constriction by triggering Ca^{2+} sparks, discrete events that initiate arterial hyperpolarization by activating large-conductance Ca^{2+}-activated K^+ channels. Micromolar Ni^{2+}, a $Ca_V3.2$ blocker, constricted pressurized rat cerebral arteries. Structural analysis revealed microdomains that comprised sarcoplasmic reticulum and caveolae, with $Ca_V3.2$ and ryanodine receptors residing next to each another. Modeling showed that Ca^{2+} influx through $Ca_V3.2$ could activate ryanodine receptors, and consistent with theory, Ca^{2+} imaging and electrophysiology demonstrated that Ni^{2+} suppressed Ca^{2+} sparks and downstream large-conductance Ca^{2+}-activated K^+ channel activity. $Ca_V3.2$ channels are also present in human cerebral arteries and drive a comparable response. In summary, we show for the first time that Ca^{2+} influx through $Ca_V3.2$ channels discretely activates Ca^{2+} sparks and large-conductance Ca^{2+}-activated K^+ channels to elicit arterial hyperpolarization and dilation. This feedback mechanism will prevent cerebral arteries from overly constricting to strong stimuli such as intravascular pressure. This new knowledge challenges the stereotypical view that Ca^{2+} channels are singularly involved in mediating arterial constriction.

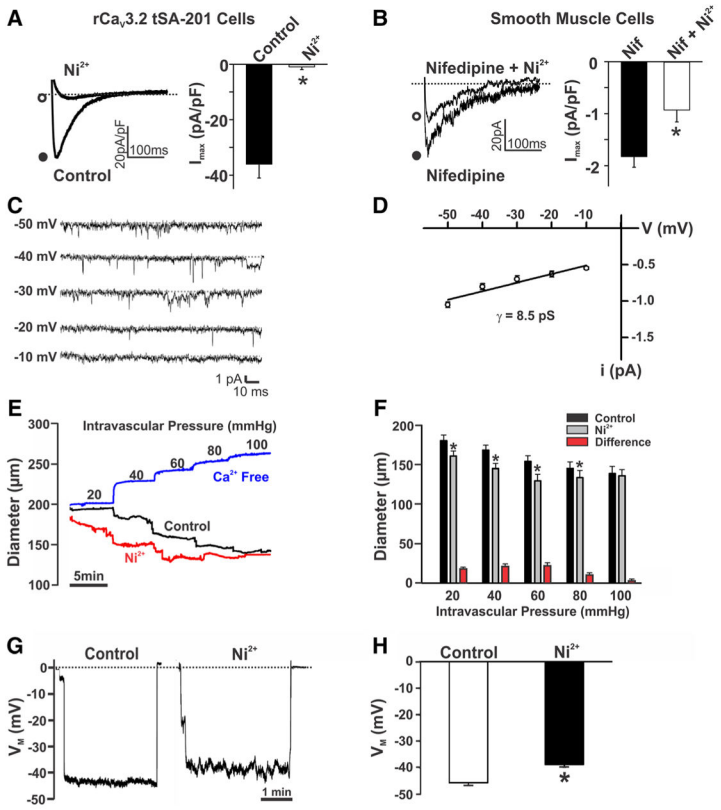

Figure 1. Effects of Ni^{2+} on $Ca_V3.2$ currents, myogenic tone, and membrane potential (V_M)

A, Representative traces and summary data of inward currents in $Ca_V3.2$-transfected tSA-201 cells in the absence and presence of Ni^{2+} ($Ca_V3.2$ blocker, 50 μmol/L). A voltage step from −90 to −10 mV was used to evoke inward Ba^{2+} current (n=5; **P*<0.05, paired *t* test). **B**, T-type current in rat cerebral arterial smooth muscle before and after Ni^{2+} (50 μmol/L). Experiments were performed in the presence of nifedipine (200 nmol/L) to block L-type Ca^{2+} channels. A voltage step from −90 to 0 mV was used to elicit inward current (n=8; **P*<0.05, paired *t* test). **C** and **D**, Single-channel recordings and summary current–voltage relationship (n=5; slope conductance=8.5 pS) of T-type Ca^{2+} currents in cerebral arterial myocytes. On-cell recording was performed at −50 to −10 mV in the presence of nifedipine (200 nmol/L), 60 mmol/L Ca^{2+}, and 50 mmol/L TEA-Cl (tetraethylammonium chloride) to block K^+ channels. **E** and **F**, Rat middle or posterior cerebral arteries were pressurized from 20 to 100 mm Hg, whereas diameter was monitored under control conditions, in the presence of Ni^{2+} (50 μmol/L) and in Ca^{2+}-free medium. Representative traces (**E**) and summary data (**F**) display augmented arterial tone in response to Ni^{2+} (n=7; **P*<0.05, paired *t* test). **G** and **H**, Arterial V_M in pressurized cerebral arteries (60 mm Hg) in the absence and presence of Ni^{2+} (50 μmol/L). Illustrative traces (**G**) and summary data (**H**) reveal the depolarizing effect of Ni^{2+} (n=6; **P*<0.05, paired *t* test).

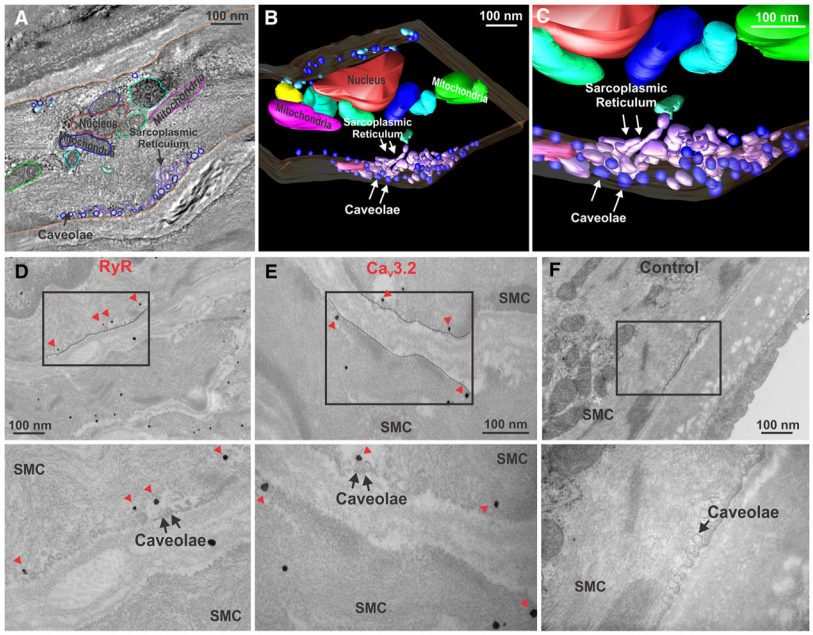

Figure 2. Electron microscopic imaging of rat cerebral arterial smooth muscle cells (SMCs)

A, Tissue sections (300 nm thick) were used to generate a contiguous stack of 2-dimensional photomicrographs (≈3.5 nm resolution); subcellular structures were subsequently traced on each section. **B** and **C**, Three-dimensional models of discrete membranous regions where caveolae and sarcoplasmic reticulum are in close apposition to one another. **D** and **E**, Transmission electron microscopy and immunogold labeling of ryanodine receptor (RyR; **D**) or $Ca_V3.2$ channels (**E**) in rat cerebral arteries. RyR labeling (arrowheads) can be observed in membranes localized beneath the plasma membrane. $Ca_V3.2$ labeling (arrowheads) was confined to the plasma membrane in association with caveolae. Boxed areas were magnified in the lower micrographs. **F**, Control experiments showed no electron-dense particles. Each photomicrograph is representative of 3 independent preparations.

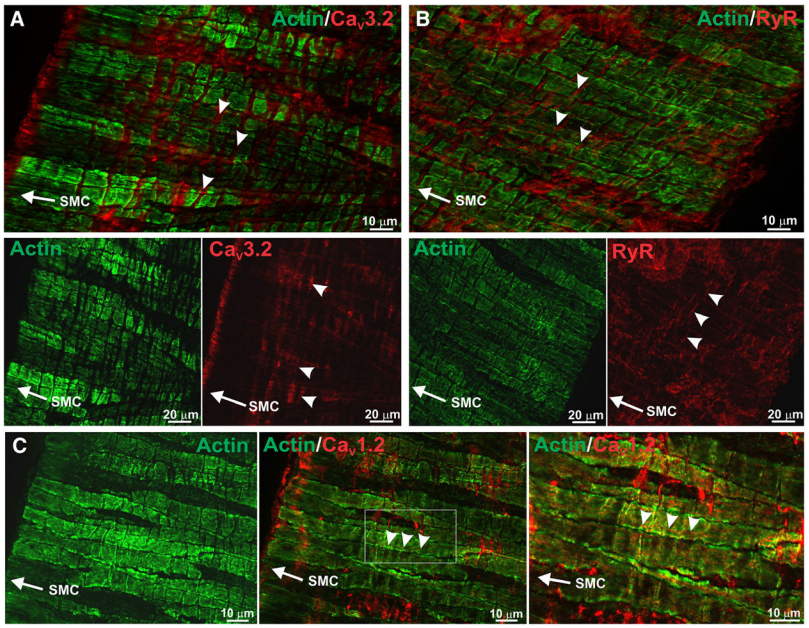

Figure 3. $Ca_V3.2$ displays localization patterns similar to ryanodine receptor 2 (RyR2) in rat cerebral arteries

A, Cerebral arteries were labeled with antibodies against smooth muscle actin (green) and $Ca_V3.2$ (red). Labeling of $Ca_V3.2$ ran perpendicular (arrowheads) to the longitudinal axis of smooth muscle cells (SMCs; arrow) in regions devoid of smooth muscle actin. **Bottom**, Smooth muscle actin and $Ca_V3.2$ are displayed separately. **B**, Immunohistochemical staining of RyR (red) localized to areas where actin (green) was absent. Magnified panels show RyR was perpendicular to the longitudinal axis of SMCs. **C**, $Ca_V1.2$ labeling (arrowheads) was parallel to the longitudinal axis of SMCs (arrow). **Right**, The boxed area (middle) is magnified. Photomicrographs are representative of 3 independent experiments.

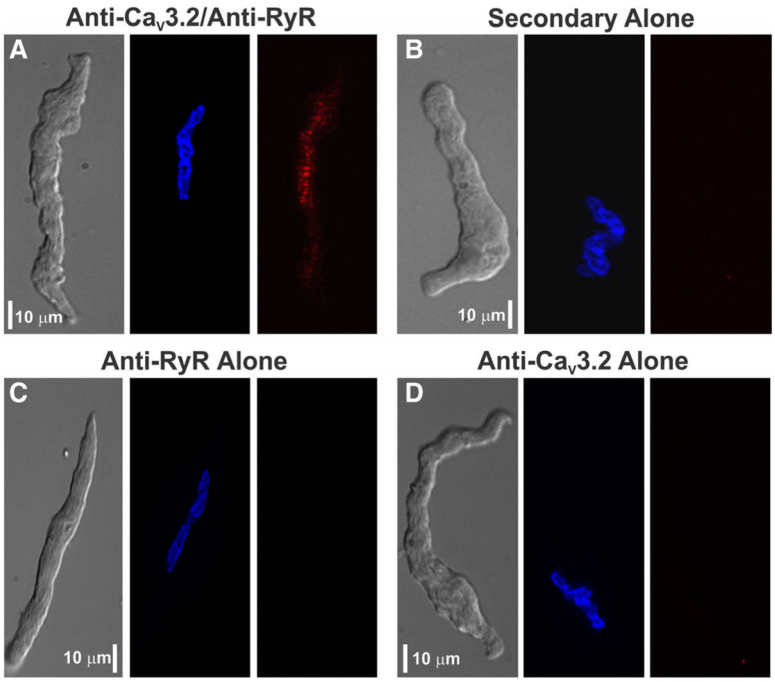

Figure 4. Proximity ligation assay of $Ca_V3.2$ and ryanodine receptor 2 (RyR2) in rat cerebral arterial smooth muscle cells

A, A gallery representation reveals the presence of red fluorescent product consistent with $Ca_V3.2$ and RyR colocalization within 40 nm of one another. Nuclei were labeled with Hoechst 33342 (blue). **B**, Assay was performed with no primary antibodies. **C** and **D**, Assay controls were developed with 1 primary antibody. Scale bars are 10 μm, and optical section depth in each image is 0.3 to 0.5 μm. Photomicrographs are representative of ≈10 to 20 smooth muscle cells, and the assay was tested 2 to 3 times for each panel.

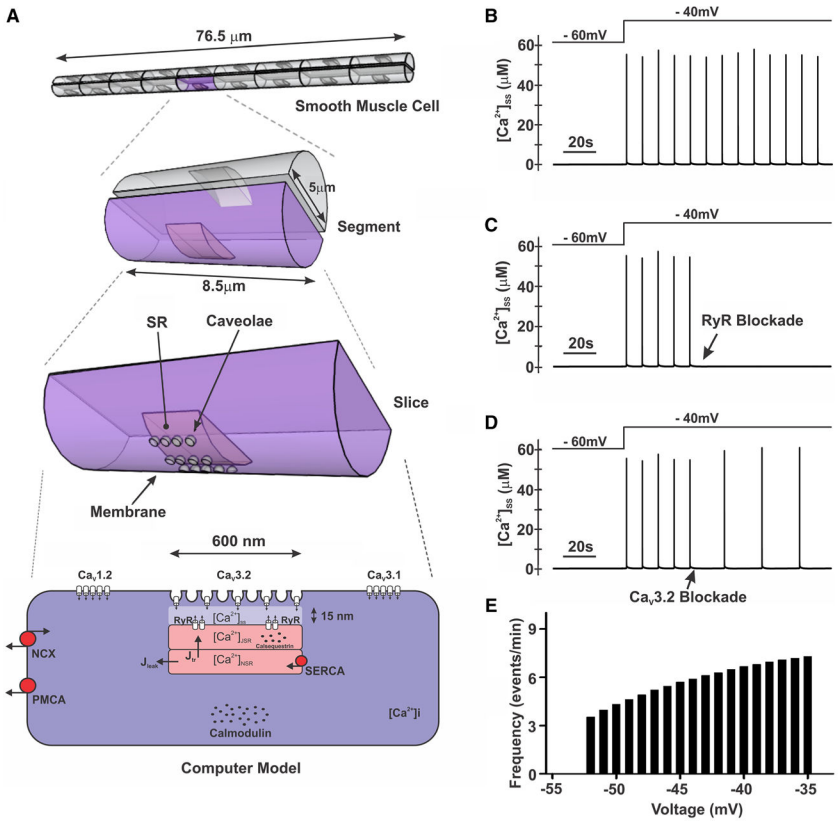

Figure 5. Computational modeling of the role of $Ca_V3.2$ in smooth muscle Ca^{2+} dynamics

A, A computational model was developed using structural and electrophysiological data. The model consists of an 8.5-μm slice of an arterial smooth muscle cell. The microdomain is 600 nm in length and 15 nm from the sarcoplasmic reticulum (SR). Membrane proteins have been distributed, and the level of expression was set by optimization procedures. Key proteins include $Ca_V1.2$, $Ca_V3.1$, $Ca_V3.2$, ryanodine receptor (RyR), Na^+/ Ca^{2+} exchanger (NCX), SERCA (sarco/endoplasmic reticulum Ca^{2+} ATPase)/PMCA (plasma membrane Ca^{2+} ATPase) pumps, calmodulin, and calsequestrin. Concentration of Ca^{2+} was calculated in the subspace region ($[Ca^{2+}]_{ss}$). **B**, Simulations display repetitive Ca^{2+} spark-like events in response to depolarization from −60 to −40 mV. **C** and **D**, Spark-like events were fully abolished by RyR inhibition and attenuated by $Ca_V3.2$ blockade. **E**, Frequency of Ca^{2+} sparks increased with depolarization.

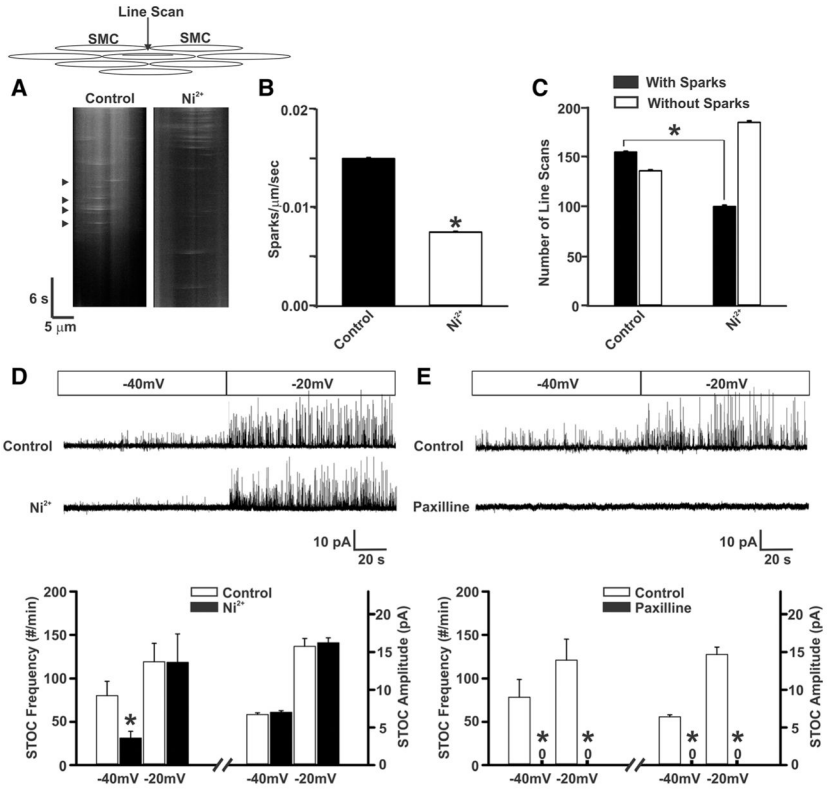

Figure 6. $Ca_V3.2$ suppression attenuates the generation of Ca^{2+} sparks and spontaneous transient outward K^+ currents (STOCs)

A, Line scan imaging performed on posterior and middle rat cerebral arteries to ascertain Ca^{2+} spark generation under control conditions and in the presence of Ni^{2+} (50 μmol/L). Arrowheads denote the presence of Ca^{2+} sparks. **B** and **C**, Summary data highlight Ca^{2+} sparks frequency (sparks/μm per second) and the number of line scans in which Ca^{2+} sparks were detected (n=6 arteries, 291 line scans in total; **P*<0.05, paired *t* test). **D**, Representative traces and summary data of STOC measurements under control conditions and in the presence of Ni^{2+} (50 μmol/L; n=8; **P*<0.05, paired *t* test). Holding membrane potentials were set at −40 or −20 mV. **E**, STOCs were monitored before and after the application of paxilline (1 μmol/L; n=8; **P*<0.05, paired *t* test). SMC indicates smooth muscle cell.

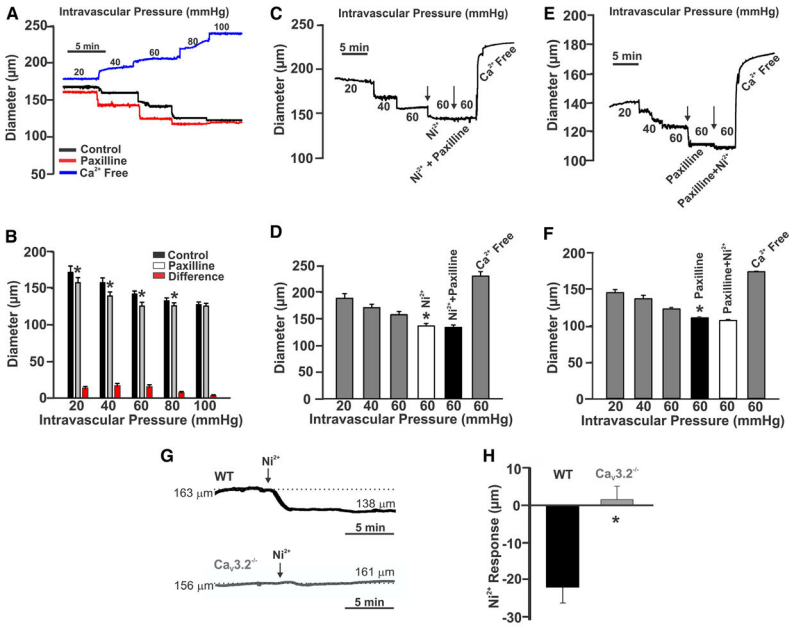

Figure 7. Effects of Ni^{2+} and paxilline on myogenic tone in rat cerebral arteries

A, Middle and posterior cerebral arteries were gradually pressurized from 20 to 100 mm Hg while diameter was monitored. The experiment was performed under control conditions and in the presence of paxilline (1 μmol/L) or in Ca^{2+}-free media. **B**, Summary data of the experiment in **A** (n=6; **P*<0.05, paired *t* test). **C** and **D**, Traces and summary data illustrate the effects of sequential exposure to Ni^{2+} (50 μmol/L) followed by paxilline (1 μmol/L; n=7; **P*<0.05, paired *t* test). **E** and **F**, The order of Ni^{2+} and paxilline in **C** was reversed (n=6; **P*<0.05, paired *t* test). **G** and **H**, Traces and summary data illustrate the effects of Ni^{2+} (50 μmol/L) on pressurized mesenteric arteries (60 mm Hg) from wild-type (WT; n=4) and $Ca_V3.2$ knockout (n=6) mice (**P*<0.05, unpaired *t* test).

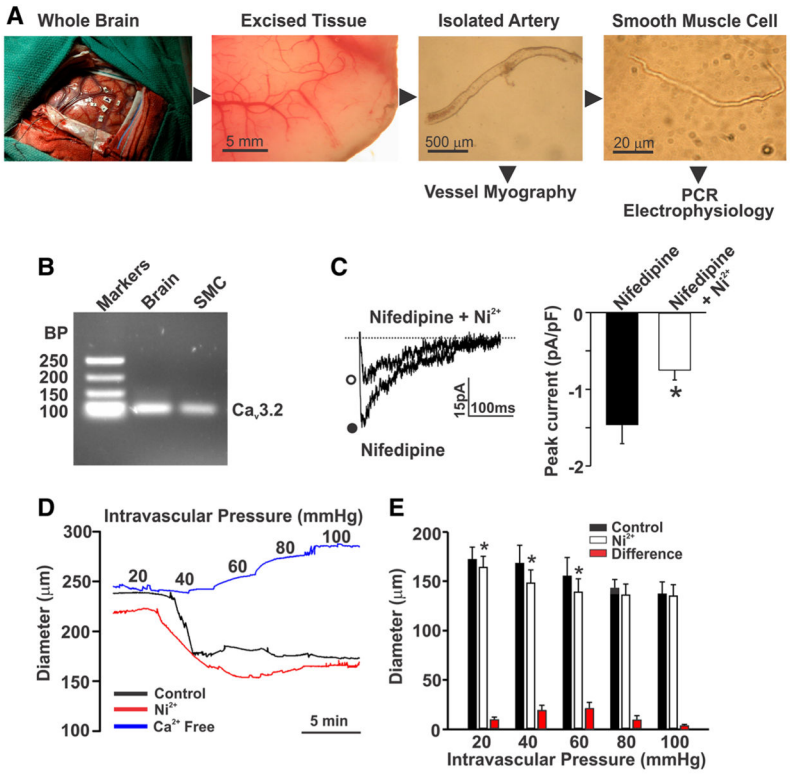

Figure 8. Expression and function of $Ca_V3.2$ in human cerebral arteries

A, Brain tissues were excised from patients undergoing lobectomy. Whole cerebral arteries and cerebral arterial smooth muscle cells (SMCs) were subsequently isolated for experimental assessments. **B**, Polymerase chain reaction (PCR) analysis of whole brain and isolated SMCs highlights the presence of $Ca_V3.2$. Data are representative of cells obtained from 2 human subjects. **C**, A voltage step from −90 to 0 mV was used to monitor inward Ba^{2+} current (n=6 cells from 4 subjects) in human cerebral arterial SMCs in the absence or presence of Ni^{2+} (50 μmol/L; **P*<0.05, paired *t* test). Currents were monitored in the presence of nifedipine (200 nmol/L) to block L-type Ca^{2+} channels. **D** and **E**, Human cerebral arteries were pressurized from 20 to 100 mm Hg while diameter was sequentially monitored under control conditions and in the presence of Ni^{2+} (50 μmol/L) or in Ca^{2+}-free media (n=4 arteries from 3 subjects; **P*<0.05, paired *t* test). BP indicates base pairs.